

Leakage currents outside an imploding Z pinch

R. E. Terry

Naval Research Laboratory, Washington, DC 20375

N. R. Pereira

Berkeley Research Associates, Springfield, Virginia 22150

(Received 7 June 1989; accepted 24 August 1990)

Leakage currents outside a pulse-line-driven Z pinch are considered in two circumstances. In the initial stage of the pinch a non-neutral electron flow can arise before magnetic insulation is established. The relative importance of such currents is estimated in terms of diode impedance and pulse-line dimensions. In the later stages of the pinch a neutralized current flow can arise in any tenuous plasma that may be present in the pinch periphery. The effects of the neutral current are estimated through self-similar solutions to a gyrokinetic equation. The collisionless plasma corona can contain an important fraction of the implosion energy.

I. INTRODUCTION

An imploding Z pinch can be used to generate large amounts of kilovolt x rays.¹ In the region of interest the yield in kilovolt x rays is roughly proportional to the fourth power of the peak current into the diode,² in agreement with theory.³ The models assume that the current density in the pinch is constant, and that all the current that goes into the diode flows through the pinch. It is very difficult to confirm experimentally that no current flows outside the Z pinch. However, the strong dependence of x-ray yield on the current implies that a small current leakage through the pinch periphery could reduce the pinch's x-radiation efficiency substantially.

In this paper we consider the leakage current outside a Z pinch in two circumstances. One is a non-neutral electron flow in the initial stage of the pinch; the other is a neutralized current flow in a tenuous plasma that may be present in the pinch periphery.

The non-neutral electron flow at the start of the pulse comes from the onset of magnetic insulation. For relevant parameters (e.g., $I \approx 1$ MA and pinch radius $r \approx 1$ cm) the magnetic field in the vacuum outside the pinch is approximately 20 T (200 kG), sufficiently strong to provide magnetic insulation. However, magnetic insulation needs some time to become established. In high-impedance vacuum transmission lines a small current pulse⁴ is seen at the front end of the pulse, and a similar transient may have been observed in a low-impedance Z pinch.⁵ Subsequently the current becomes sufficiently large to cut off this transient. According to our computer simulations the transient current is composed of an electron sheath that is captured by the magnetic field. When magnetic insulation sets in the electron sheath rolls up into relatively stable vortices.

The neutralized current flow in the pinch periphery would take place at a later time, during pinch compression. In the initial stage of the pulse the material in the diode is rapidly ionized, a complicated process outside the scope of this work. The current compresses the bulk of the material, which becomes a dense collisional plasma that is accelerated toward the axis. The behavior of this plasma is described by the resistive radiation-hyromagnetic equations.⁶ However,

in computations with these equations⁷ the exterior of the plasma sometimes becomes too conductive in an unphysical way—the plasma temperature T as computed can exceed 100 keV. In this case the standard Spitzer formula for the conductivity σ in a collisional plasma, $\sigma \propto T^{3/2}$, predicts a highly conductive plasma in the pinch periphery that prevents the current from entering the Z pinch. The problem disappears when the currents in the plasma periphery are computed by keeping account of the transition from a plasma dominated by collisions to a collisionless plasma. For practical purposes the plasma becomes collisionless when the electron–electron collision time exceeds a typical hydrodynamic time scale.

In the strongly magnetized collisionless exterior plasma the standard equations of resistive hydrodynamics are not valid. Instead, the plasma electrons drift in the confining magnetic field $B_\theta(r)$ and the combined applied and space-charge electric field $\mathbf{E} = [E_z(z,r), E_r(z,r)]$. The $E_z \times B_\theta$ drift inward generally dominates. The current density J_z no longer satisfies Ohm's law, but can be derived by setting the power density $J_z \cdot E_z$ equal to the change in kinetic energy density.

The collisional core of the Z pinch implodes differently than the plasma periphery. In the core the collisions guarantee an isotropic velocity distribution, and an isotropic pressure, but in the periphery the electrons conserve their angular momentum p_θ as they travel along the magnetic field lines around the pinch axis. As the radius r decreases the electron velocity v_θ increases as $1/r$, and the parallel pressure $P_\parallel \propto v_\theta^2$ increases as $1/r^2$. Also, the magnetic moment around the magnetic field, $\mu \propto mv_\perp^2/B_\theta$, is conserved. Therefore the perpendicular pressure $P_\perp \propto v_\perp^2$ increases linearly with the magnetic field $B_\theta(r)$, which is proportional to $1/r$. The ratio of parallel to perpendicular components of the pressure, $P_\parallel/P_\perp \propto r^{-1}$, can become important.

A simple estimate for any peripheral current can be obtained from the Bennett relation applied separately to the core and the periphery. One has $I^2 \sim NT$, with I the current, N the line density of the particles, and T the temperature. Therefore, in order of magnitude $I_{\text{peri}}/I_{\text{core}} \sim (N_{\text{peri}} T_{\text{peri}}/N_{\text{core}} T_{\text{core}})^{1/2}$, where $N_{\text{core(per)}}$ is the number

of particles in the core (periphery) of the pinch, $T_{\text{core(per)}} is the applicable temperature, and $I_{\text{total}} = I_{\text{peri}} + I_{\text{core}}$.$

A reasonable mass per unit length for the core of the Z pinch is perhaps $100 \mu\text{g}/\text{cm}$. The initial particle density in the Z-pinch periphery is on the order of $n \approx 10^{13}/\text{cm}^3$ (for 0.1 Pa or 1 mTorr), spread over, perhaps, 100 cm^2 . The mass per unit length on the outside of the pinch is thus $\sim 0.01 \mu\text{g}/\text{cm}$. Setting the typical temperatures about equal suggests a relative current loss of $\sim 1\%$ in such an equilibrium, which is negligible. However, when $T_{\text{peri}} \gg T_{\text{core}}$ after compression of the periphery, and/or when pressure balance is not applicable, the current loss through the periphery may become larger.

In Sec. III of this paper we treat current conduction through the periphery with the gyrokinetic formulation of Bernstein and Catto.⁸ This model is obtained from the single-particle kinetic equation by introducing higher-order accurate invariants in the velocity space and then averaging over the gyrophase. We employ a current density obtained from the velocity moment equation of this gyrokinetic formulation, which expresses the momentum balance between particles and fields. The current density then involves a pressure tensor.

Analogous to self-similar hydromagnetic flows⁹ with scalar pressure, the gyrokinetic momentum equation also admits self-similar distribution function solutions that exhibit tensor pressure. If $P_{\parallel} \neq P_{\perp}$ these special solutions remain separable but exhibit three characteristic frequencies instead of two, and, when we retain displacement current, a fourth frequency is added. A particular example from the self-similar theory is used here to illustrate the effects of peripheral gyrokinetic plasma, future work will discuss these solutions in more depth.

The retention of displacement current is required for the energy transport from an external circuit through the vacuum region to the plasma load. The principal consequence is that the well-known plasma dielectric constant $\epsilon \sim (1 + c^2/c_A^2)^{1/2}$ becomes significant (c_A is the Alfvén speed). The plasma dielectric, the radial acceleration of plasma mass, and the two tensor pressure components provide a four-fold energy sink between the core plasma load and the external driver circuit.

II. ESTABLISHMENT OF MAGNETIC INSULATION AROUND A Z PINCH

In the initial stage of the pinch all material is contained in the conductor, and outside of the conductor is vacuum. Free electron current in the diode can be computed with a particle in cell code. One computation uses the geometry of Fig. 1, which is typical for Z pinches. The cathode is a cylinder with radius 3.4 cm, inside an anode with radius 5 cm, and a 3 cm wide anode-cathode gap forming the diode. The diode is bridged by an ideal conductor that mimics the Z pinch. The Z pinch radius, 0.6 cm, is representative of multiple wire loads but substantially smaller than the initial radius of a gas puff. Electrons can be emitted from the cathode surfaces as indicated. The emission assumes space-charge limited flow, i.e., electron emission continues until the normal electric field vanishes. Ions are ignored in our computations.

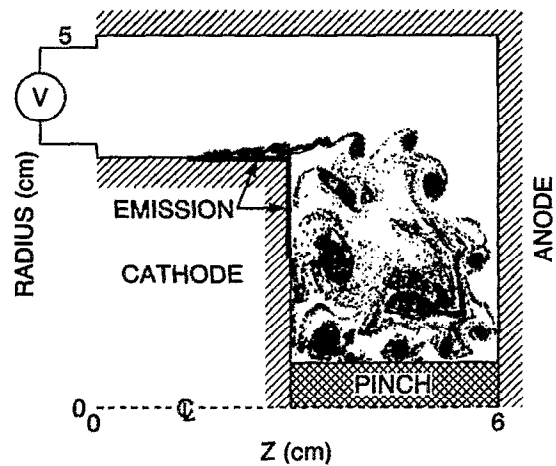


FIG. 1. Geometry of the Z-pinch diode as used in the computation. The cathode is a cylinder of radius 3.4 cm at 3 cm away from an anode with radius 5 cm. The Z pinch is mocked up as a 0.6 cm radius conductor that connects cathode and anode. The electron emission surfaces are indicated on the cathode. The voltage source is connected at the entrance of the diode, 6 cm away from the anode plane. Initially the diode vacuum contains no electrons: The figure shows the electron positions at 4.4 nsec into the simulation.

Figure 2 is the assumed electrical pulse at the diode. The voltage rises linearly on a 5 nsec time scale to over 1 MV. The current is quadratic in time in agreement with $\dot{I} = V/L$. At the end of the simulation the current exceeds 100 kA, for a magnetic field at the Z-pinch edge up to about 4 T (40 kG). The current in free electrons is the lowest line in Fig. 2. The current starts once the electric field in the diode feed exceeds the field emission threshold, taken to be 200 kV/cm in the code. This occurs at about 1.5 nsec.

When the first electrons are emitted the current through the Z pinch is only 15 kA, insufficient for magnetic insulation. Therefore the free electrons simply cross the diode gap. Later in time these electrons become trapped by the magnetic field from the Z-pinch current. These intermediate stages are not shown, but they can be inferred from Fig. 1, which

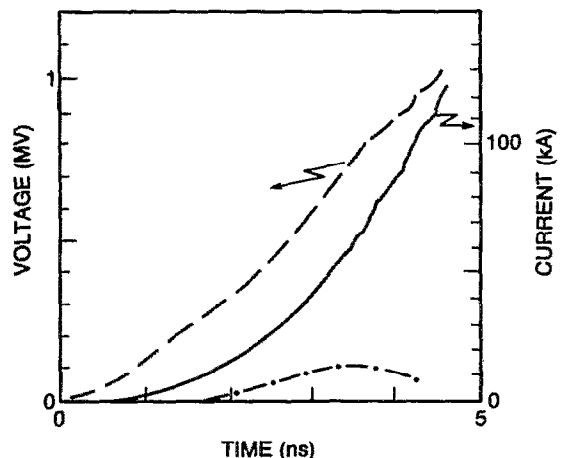


FIG. 2. The voltage V and the current I of the electrical pulse at the diode entrance. The dashed line at the bottom gives the leakage current in free electrons coming off the cathode shank.

shows the distribution of free electrons at the end of the run. The magnetically insulated space-charge sheath in the current feed appears to stream off the cathode into the diode already filled with electrons emitted previously. The sheath is clearly unstable, rolling up into vortex-like structures that persist as they move toward the center conductor.

There is an exact analogy between strongly magnetized non-neutral electron beams and inviscid fluid flow.¹⁰⁻¹³ In two-dimensional Cartesian geometry with constant magnetic field B_z , the combination of charge density, permittivity, and magnetic field in the form $\rho/\epsilon_0 B_z$ corresponds to the vorticity $\zeta_z = \nabla \times \mathbf{U}_D$, where \mathbf{U}_D is the two-dimensional drift velocity. This drift velocity U_D can be derived from the streamfunction ψ as $\mathbf{U}_D = (-\partial\psi/\partial y, \partial\psi/\partial x)$, where $\nabla^2\psi = \zeta_z$.

The exact correspondence breaks down in cylindrical geometry because the magnetic field varies with radius, $B_\theta = \mu_0 I / 2\pi r$; now

$$\nabla \times \mathbf{U}_D = \frac{-\rho}{\epsilon_0 B_\theta} - E_r \frac{\partial(1/B_\theta)}{\partial r}. \quad (1)$$

The last term is small compared to the first, except perhaps near the central conductor, where the blob size is comparable to the geometrical scale. Hence in our diode the analogy with inviscid shear flow is largely valid.

The magnetically insulated space-charge sheath coming off the cathode is then analogous to a vortex sheath. It is well known that such a sheath is unstable, and that the instability develops into coherent vortex regions reminiscent of the space-charge blobs seen in our simulation. It is also known that the vortex regions are relatively stable, similar to the persistence of our blobs. Furthermore, interaction between the blobs can be treated as the motion of two-dimensional vortex lines.

The electron blobs appear to be self-contained entities, consistent with $E \times B$ drift motion for the strongly magnetized electrons in the blob's space-charge field. In this case the blob electrons remain on equipotential lines, since the drift is perpendicular to the potential gradient, $(\mathbf{E} \times \mathbf{B}) \cdot \mathbf{E} = 0$. In a cylindrically symmetric blob the charge convected by the drifting electrons is then invariant, and the blob is a stationary entity. Qualitatively similar results are found in simulations with other parameters, e.g., a slower voltage rise time, or a smaller Z-pinch inductance more representative of a gas puff.

The leakage current in free electrons for the run in Fig. 2 peaks at 15 kA around 3.5 nsec, and decreases thereafter. At these later times the current is magnetically insulated, and its magnitude can be estimated by considering the drift current in the thin space-charge sheath parallel to the cathode shank (see Fig. 1). The current in the detached blobs can be considered equal to that flowing along the cathode shank since there are no sources or sinks in the detachment region.

In an insulating magnetic field B_θ the sheath electrons drift in the axial direction along the cathode shank with drift velocity $U_z \approx E_r \times B_\theta / B_\theta^2$. The electric field varies throughout the electron sheath from zero at the metal surface of the cathode to E_r at the top of the sheath, but the magnetic field is mainly from the central current; hence $B_\theta \approx \mu_0 I / 2\pi r_i$.

The current in the electron sheath I_e is then approximately $I_e \approx 2\pi r_i \sigma U_z$. The surface charge density σ of the cathode sheath is $\sigma = \epsilon_0 E_r$, where E_r is the normal electric field at the outside of the electron sheath. Since the sheath is thin compared to the width d of the pulse line, and d is less than the inner radius r_i , the electric field can be approximated by $E_r \approx V/d$. Usually the rise time τ is so fast that the voltage can be approximated by the inductive voltage $V \approx LI/\tau$, with L the diode inductance and I the total diode current.

The relative importance of early free electron leakage current to the total pulse line current then becomes

$$\frac{I_e}{I} \approx \left(\frac{E_r}{cB}\right)^2 \approx \left(\frac{r_i}{d}\right)^2 \left(\frac{Z_D}{Z_0/2\pi}\right)^2, \quad (2)$$

where $Z_0 = (\mu_0/\epsilon_0)^{1/2} = \mu_0 c = 377 \Omega$, and $Z_D = V/I \approx L/\tau$ is the total diode impedance. After magnetic insulation is established in the pulse line this leakage current decays away.

The literature on magnetic insulation¹⁴⁻¹⁷ contains estimates along the same lines as the above. In addition, it is shown in detail that the single-particle considerations used here correspond well to a treatment that includes the self-electric and self-magnetic fields.

A typical Z-pinch diode is about 3 cm wide, and the inductance $L \approx 6$ nH. A typical pulse rise time may be ≈ 12 nsec, for a diode impedance of about 0.5Ω . In contrast, the vacuum impedance $Z_0/2\pi = 60 \Omega$, and the impedance ratio is $\frac{1}{100}$. The leakage electron current I_e is thus always a small fraction of the total current I , whence I_e can be ignored.

However, for single exploding wires the vacuum current may become comparable to the conduction current. As an example, the inductance of a single $25 \mu\text{m}$ radius wire load in a 3 cm wide diode is about 45 nH. For a fast (10 nsec) rise time pulse the factor $Z_D/Z_0 \approx 0.1$, but a relatively small gap size partly compensates. When $r_i/d \approx 3$, for example, I_e/I is of the order $\frac{1}{10}$. In this case there should be a sizable leakage current in free electrons, potentially generating a measurable⁵ bremsstrahlung x-ray signal. If corroborated by further work the bremsstrahlung x-ray signal may be an excellent indicator for the arrival time of the electrical pulse at the Z pinch.

III. COLLISIONLESS PLASMA PERIPHERY

Once magnetic insulation has been established, as discussed in Sec. II, the current flows principally through the pinch, and the pinch accelerates inward. Eventually the pinch stagnates on axis, forming a dense, current-carrying cylinder of plasma. However, this pinch core could be surrounded by a periphery of collisionless plasma, from Z-pinch material that did not fully implode or from background gas that was swept in from the outer regions of the diode. In this section we consider the current that might be carried by such a plasma.

The peripheral plasma might be different in Z pinches that start from an injected gas on one hand, and multiple wires on the other. The injected gas forms a plume with the highest density opposite the nozzle opening, and wide wings of decreasing density. The initial breakdown and current conduction should occur along the spatial contour in the

diode, which (given the electric field and material profiles) is at the minimum of the Paschen curve, and thus should leave some gas outside the initial current channel. This gas may be ionized later to form the periphery. With wires the exterior plasma would come from the early blowoff as the wire load is heated, or it might not exist at all. The ambient gas in the diode can be another source of tenuous plasma, perhaps resulting in ion densities as high as $10^{12}/\text{cm}^3$ (and electron densities $<10^{13}/\text{cm}^3$).

Ironically, sometimes¹⁸ there is current leakage through a tenuous plasma on axis inside the wires: when the wires are heavy the outer part of the wire is shed continuously throughout the current pulse. This plasma implodes on axis before the original wires have moved, and diverts part of the current.

More recent wire load implosions¹⁹⁻²¹ involving Ni arrays indicate a fairly weak inductive current notch and radiation emission peaking after the plasma starts to expand. When the diode energy flow is examined the energy input to the load from classical Ohmic heating and inductance change is apparently insufficient to account for the total energy radiated. Some energy must be removed from the vacuum magnetic field in order to account for the discrepancy. Now such an analysis is not supported by an independent measure of the current distribution in the pinch; indeed, the location of the current path is simply taken as the boundary of luminosity in pinhole photos. Should the current flow deeper in the plasma so that the peak compression is greater, then some improvement in the energy discrepancy would be realized insofar as the effective inductance change would be larger. Yet it is difficult to account for the energy by this effect alone because the current path would have to be very deep (≈ 0.01 mm). Such a current filament would be much thinner, in fact, than the observed (Ni) *L*-shell emission filament. If, however, the outer load regions are in a gyrokinetic coronal limit, as described below, then the work done on the gyrokinetic plasma would be absorbed from the vacuum magnetic field and at least partially transferred to the interior pinch after stagnation. In consonance with observation, such motion would not provide much of an inductive current notch, because of the ability of this coronal plasma to hold a more constant current while a load stagnation occurs.

Moreover, comparing theoretical and experimental energy coupling to Ar gas puffs provides further indirect evidence of exterior energy sinks, which could be tenuous peripheral plasma. The work of Thornhill²² suggests that lower mass puff loads exhibit radiative *K*-shell yields lower than expected if all the energy transferred to the load cavity was, in fact, coupled to the central plasma load. The experimental yields were more heavily weighted to the *L* shell, suggesting a lower load temperature at stagnation—even though the puff gas load accepted more generator energy than the hydromagnetic calculations could predict. This is again precisely what would be expected should an intervening energy sink arise in the load periphery and “soften” the implosion.

In contrast, more recent gas puff implosions²³ show a fairly pronounced inductive current notches as little as 5 cm from the load. The design changes to the gas puff load were quite substantial in comparison to the experiment studied by

Thornhill. In Spielman's experiment the puff mass was much larger, the front end inductance was reduced, the neutral flow speed was increased to Mach 8 (rather than Mach 4), and the return current anode plane was both a somewhat thinner wire mesh and closer to the cathode. It would appear that the energy transfer was quite efficient, perhaps indicating that coronal plasma was either absent or if present not behaving as a strong energy sink. The best data presently available cannot resolve these possibilities.

Hence there is a good reason to believe that only a detailed examination of the differences in behavior between gas puffs and imploding wires would contain some direct evidence for current leakage throughout a peripheral plasma. The differences to be examined must rest upon clear measures of the load mass in a gas puff, which is not generally available, and good measures of energy flow in the diode region. If corona plasma is produced mostly from background gas, then no major wire/puff differences would be expected. If the corona plasma in gas puffs is due to an incomplete sweep-up of the load gas, then wire/puff differences would depend on the actual puff load mass (and its distribution) as compared to the extent (and distribution) of any early wire blowoff.

The remainder of this paper assumes that the Z-pinch periphery contains a collisionless plasma, with density and temperature fixed to values within the known experimental and theoretical limits. For the number and energy densities one could reasonably associate with such a “test” plasma, a simple calculation will show how the peripheral plasma can become important for Z-pinch implosions.

What is the current density in the collisionless periphery surrounding the current carrying Z pinch? In a dense plasma the collisions are the dominant influence balancing the motion of the plasma electrons against the acceleration by the electric field. The resulting collisional electron drift, and thus the current density J is proportional to the electric field E , $J = \sigma E$. The electrical power input into the plasma ends up in increased random velocities of the plasma particles, viz., Ohmic heating.

In the absence of collisions the magnetized plasma in the Z-pinch periphery can absorb energy from the electrical pulse. In this case the energy does not go into random motion of the plasma particles, but instead is put into organized motion. A strongly magnetized plasma in an electric field is not accelerated along the field, but drifts perpendicular to the electric and magnetic fields with a velocity $W = cU = -(E/B)$. For constant E the drift speed remains constant, but when the electric field increases in time the plasma accelerates. The kinetic energy density $\mathcal{E} = \rho W^2/2$ increases (ρ denotes the plasma mass density) and electrical power is absorbed. Likewise, electrons that $E \times B$ drift into a region of increased magnetic field spin up, increasing their perpendicular energy w_\perp while the magnetic moment $\mu \sim w_\perp/B$ stays constant. The increase in w_\perp , or the increased magnetization, is another power sink. In a cylindrically symmetric geometry with $B \sim 1/r$ the particle's angular momentum about the axis, $p_\theta = mrv_\theta$, is conserved; therefore a drift toward the axis increases the parallel energy w_\parallel as $1/r^2$. Further details of the description are developed

in the Appendix, where it is shown how special solutions of the gyrokinetic equation can be used to model the coronal plasma.

In particular, the limit of homogeneous compression and special initial conditions allows the solutions to simplify. The dependent variables and their derivatives are then functions of the single self-similar invariant $\xi = r/r_* \alpha(\tau)$. Here $r_* = r_*/l_0$ is a dimensionless scale length that arises naturally in the theory with $ct_0 = l_0$ and $\tau = t/t_0$. The time scale t_0 is tied to a particular implosion time scale. The variable $\alpha(\tau)$ contains the sole time dependence, e.g., $U = \dot{\alpha}r_0$, $DU/D\tau = \ddot{\alpha}r_0$. Four primary frequencies arise. The oscillatory frequency is related to the magnetic field pressure; $\tau_A = \omega_A^{-1}$ is the transit time of an Alfvén wave with velocity c_A through the pinch scale length. Two new frequencies, expressed as ratios of thermal velocities to light speed, are related to the anisotropy. The parallel pressure frequency is $\omega_{\parallel}^2 \equiv c_{\parallel}^2/c^2$, and the perpendicular pressure frequency, $\omega_{\perp}^2 \equiv c_{\perp}^2/c^2$. The displacement current frequency, $\tau_E = \omega_E^{-1}$ is a measure of the overall dielectric strength characterizing any particular flow.

To assess the role of this sort of collisionless current channel in the evolution of a Z pinch, we select a set of self-similar profile functions, which is compatible with the (rather sparse) information available on the coronal plasma and examine the evolution of the special solution. In particular, what fraction of “new” current is absorbed into such a corona after it is formed under the magnetizing influence of early interior currents flowing only in the dense pinch? What fraction of the incoming energy flow from the driving circuit is diverted into this corona, and what circuit waveform behavior is characteristic of such an external plasma layer?

We can formulate these questions in a realistic context by specializing the self-similar equation of motion derived in the Appendix to portray a coronal rundown in a Z-pinch diode. Each of the four independent frequencies appearing in

$$\ddot{\alpha} = \frac{\omega_{\parallel}^2}{\alpha^3} + \frac{\omega_{\perp}^2}{\alpha^2} - \frac{\omega_A^2}{\alpha} + \frac{\omega_E^2}{\alpha} \dot{\alpha}^2$$

can be set to produce a desired result in the solution. In the example developed here ω_{\perp}^2 and ω_{\parallel}^2 are selected to correspond to $\perp(\parallel)$ temperatures of 75(60) eV, which is consistent with ionization at a few electron volts and subsequent Ohmic heating by about a factor 10 before a “collisionless” state is obtained.²⁴ This leaves ω_E^2, ω_A^2 , a radial extent $[\xi_-, \xi_+]$, and an initial velocity $U(\xi_+)$ to be developed. Since $r_* = \omega_E/\omega_A = U(\xi_+)/\dot{\alpha}_0$, the selection of either $\dot{\alpha}_0$ or $U(\xi_+)$ ($\approx 7.33 \times 10^7$ cm/sec) is, for fixed r_* , guided by the typical collapse time of pinch loads, taken here to be about 30 nsec over a radial extent of 1.5 cm. In keeping with common pinch diode dimensions, the radial extent of the corona is taken to be ≈ 4 cm. Hence the values for ξ_- and ξ_+ will correspond to $\xi_- = 1.5 \text{ cm}/l_0 r_*$, $\xi_+ = 5.5 \text{ cm}/l_0 r_*$; $l_0 = 30$ cm, since the collapse time is in the nanosecond range.

The value inferred for r_* must be guided by the densities implied for the profile. With an upper limit of 10^{15} ions/cm³, suggested by the lower limit of schlieren measurements, values of r_* on the order of [0.25, 0.312] keep the

density bounded above by this constraint when the density scale $n_0 = (2.366 \times 10^9/A) [\dot{\alpha}_0/U(\xi_+)]^2 (I_{\text{core}}/1 \text{ MA})^2$ (cm⁻³), and the density profile

$$n(\xi) = \frac{n_0}{\xi^2} \left(\frac{\tau_E^2}{1 - \xi^2} - 1 \right) \times \left(\frac{1}{\sqrt{1 - \xi^2}} - \frac{1}{\sqrt{1 - \xi_-^2}} + 1 \right)^2, \quad (3a)$$

are evaluated for an enclosed current $I(\xi) = I_{\text{core}} \cdot (1/\sqrt{1 - \xi^2} - 1/\sqrt{1 - \xi_-^2} + 1)$ of a few mega-amperes.

The selection of r_* to set the density leaves arbitrary the choice of either ω_E or ω_A . For this example the selection of a moderately strong dielectric coefficient,

$$\epsilon(\xi)/\epsilon_0 = \tau_E/\sqrt{1 - \xi^2} \quad (3b)$$

(peaking at about 150 ϵ_0) implies, together with r_* , a value for ω_A . Similar expressions for the temperature profiles are easily derived from Eqs. (A9b) and (A9c).

Such a group of solutions is shown in Fig. 3. To summarize, initially the interior boundary of the solution domain is given a velocity of 2.0×10^7 (cm/sec), which corresponds to a typical peak implosion velocity of Z-pinch loads in machines of moderate energy. The interior coronal (H^+) ion density is about 1.04×10^{15} cm⁻³ per MA² of interior current; it extends for 4 cm outside the interior radius of 1.5 cm. [The factor MA² is obtained from Eq. (3a), in analogy to the Bennett pinch relation.] The initial coronal conduction current is 34% of the core current. The density $n(\xi)$ decays nearly $\propto 1/\xi^2$, while the perpendicular nearly h_{\perp} is nearly $\propto \xi$; Eq. (A9b) produces a parallel energy profile h_{\parallel} also nearly $\propto \xi^2$. Since c_{\parallel} is an azimuthal thermal speed at the scale radius, and since the thermal speed profile is proportional to the scale radius, the average angular momentum profile is $p_{\theta} \sim r_0 v_{\theta} \sim c_{\parallel} \xi^2 r_* l_0$ so that $L_{\parallel}^2 \sim \xi^4 (l_0 r_*)^2 c_{\parallel}^2$ as demanded by the self-similarity constraints. The net result is that the azimuthal component $P_{\parallel} = \rho L_{\parallel}^2/r^2 \propto n_0 v_{\parallel}^2$ is nearly independent of radius. The perpendicular component $\xi P_{\perp} \propto \xi n_0 v_{\perp}^2$ is also weakly dependent on radius.

The initialization conditions required to produce this sort of energy profile are not precisely known, but the fact

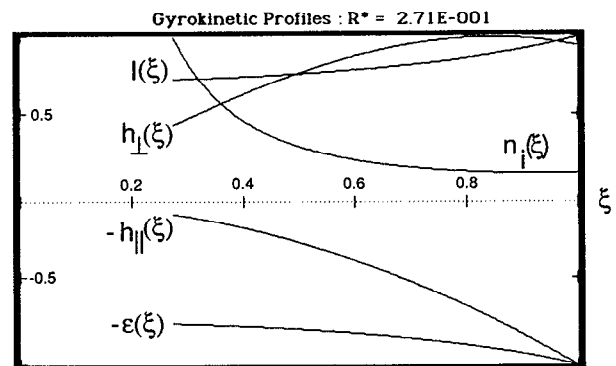


FIG. 3. Examples of initial self-similar profiles are shown. As labeled the curves are normalized to $n_0 = 1.04 \times 10^{15}$ cm⁻³ MA⁻², $I = 1.34 \times I_{\text{core}}$, $\epsilon = 150$, $h_{\parallel} = 60$ eV, and $h_{\perp} = 75$ eV.

that $P_{\parallel} \sim \xi P_1$ is consistent with a simple model for the early phase. If thin peripheral gas is photoionized and Ohmically heated while in an azimuthally directed magnetic field, then it will evolve to a collisionless state principally through electron-neutral collisions. The conductivity will smoothly evolve to a small value as runaway electrons separate in energy from the bulk electrons that interact readily with the neutrals and ions. Since the runaway electrons are captured in a radial $\mathbf{E} \times \mathbf{B}$ drift they are confined to the r - z components of the velocity space unless scattered into the θ component. The energy dumped into the r - z motion depends on the time history of the conductivity and local E_z field, but the rate of scattering into the θ direction depends on the number of scattering neutrals and ions available at any radial location. Since the number of such scattering centers in any azimuthal flux tube is linear in the radial coordinate, the power diverted to the azimuthal direction increases $\propto r$. Hence, for any particular time history of r - z heating, the final energy dumped in the θ direction will be proportionately greater at larger radius. The energy density in the r - z component is deposited in each volume independently, but at a fixed radius scattering in the whole volume swept out by a gyrating electron diverts energy to the azimuthal component.

Insofar as these self-similar flows fix the (conduction) current partition between the core and the periphery, they are only useful as approximate models of the load as it enters the final rundown and stagnation phase. At this time the interior load is expected to be hot enough to curtail further magnetic diffusion, while the peripheral plasma is forced to conserve flux unless it becomes turbulent as a result of microinstabilities. Since much of the energy transfer to a Z pinch is due to the load's inductance change, a fair fraction of this energy is transferred in the last phase of the rundown. The self-similar models can therefore offer a simple treatment of this important phase of the motion by initializing their parameters to pinch load conditions after the implosion is well underway.

The dynamic consequences for an imploding load surrounded by a coronal plasma of this sort are shown in Fig. 4. The final 30 nsec of the rundown are strongly modified by

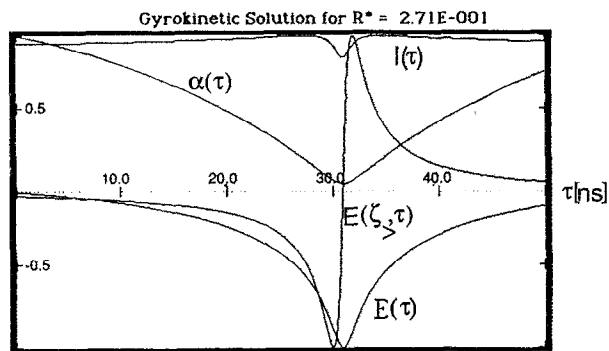


FIG. 4. Time histories of the current $I_{\text{total}}/I_{\text{core}}$, exterior electric field $E(\xi, \tau)$, radius α , and absorbed energy $E_a(\tau)$ over a 50 nsec rundown. As labeled the curves are normalized to $I = 1.45 \times I_{\text{core}}$, $E_s = 1.45$ MV/cm MA², $E_a = 143$ kJ/cm MA², and $\alpha = 1$.

the collisionless magnetoplasma corona. As the radial compression ($\sim \alpha^{-2}$) reaches its maximum, the exterior electric field reverses and the peak in the absorbed energy is obtained. While the conduction current is constant over the interval, the total current rises slightly and exhibits a very mild inductive notch. All this time dependence, about a $\pm 11\%$ current variation, is due to the displacement current, which alternately charges and discharges the plasma dielectric while a fixed conduction current leaks across the diode.

If the load were a bare slug, its motional impedance would become more important in the rundown. Further power absorption by the Z pinch would be strongly curtailed and one might expect a 30%–40% “inductive notch” to develop in the current waveform. The gyrokinetic corona has changed this picture substantially. Now further power absorption can occur, but most of the energy goes no further than the corona. The implosion and stagnation occur on a normal time scale but the interior load current is fixed. Whereas the coronal conduction current is fixed as well, the displacement current component can vary in strength from 5%–20% of the core current, depending on the strength of the plasma dielectric that has been trapped in the periphery. At fixed interior current the stronger dielectric cases tend to implode less sharply as a result of the larger mass and slower Alfvén speeds. The slower time scale implies less displacement current because the accelerations are weak. In contrast, the weaker dielectric cases provide a more prominent displacement current component because the accelerations are stronger. During the stagnation, energy is deposited in the coronal fields and matter. The energy given the coronal plasma is released when the motion reverses, as a result of the recoil of the gyrokinetic plasma from the angular momentum and magnetization stresses, which build up as the radius gets smaller and finally cannot be overcome.

In the case illustrated previously (at the time of peak compression) this diverted energy $E_a(\tau)$ has risen to 143 kJ/cm MA² of interior current. In the absence of any dissipative mechanisms this energy would be released back to the driving circuit as the plasma expands—it is never coupled to the dense portions of the load! If we evaluate the peak coronal energy for the currents and load lengths discussed in the Gamble II analysis by Thornhill, the absorption of this coronal energy into the load region would result in much more additional energy removed from the pulseline, which more than removes the energy coupling discrepancy between theory and experiment at lower load masses. If anomalous dissipation mechanisms are, in fact, active in these coronal plasmas, then this is also the rough magnitude of energy available to the load as additional heating. Such a channel would provide a path for conversion of energy in the vacuum magnetic field to the load without compression of the current filament to very small dimensions, as required to explain the observations of Ref. 19.

IV. SUMMARY AND CONCLUSIONS

Current can be lost in the periphery of a Z pinch by various mechanisms. Initially the Z pinch carries no current, and the inductive voltage at the edge of the cathode away

from the pinch material can drive a current in free electrons. The free electrons can be the bulk of the current at the very start, but this current is cut off rapidly once the current starts flowing through the Z pinch.

The tenuous plasma outside the Z pinch can also carry current. How much current is shunted through this plasma depends on the plasma density, and also on parameters such as the temperature and the magnetic field in the periphery, i.e., the current in the main Z pinch. The pressure of the collisionless plasma in the periphery becomes anisotropic as the plasma contracts toward the axis, as a result of the separate conservation of the electron's magnetic moment, and the electron's angular momentum about the axis. Under these conditions the plasma can still oscillate in a self-similar manner for a constant interior Z-pinch current. The constraint of constant interior current is also consistent with the ideal hydromagnetic self-similar flows useful in modeling the dense interior plasma. Both interior and peripheral plasma are thus modeled in a mutually consistent way. While the apportioning of current between the interior and the corona is an important issue, it is beyond the scope of this work. Here the model is built to describe the motion after the interior plasma is hot enough to curtail further magnetic diffusion, and thus a fixed interior current is the proper boundary condition.

In contrast to self-similar hydromagnetic oscillator solutions, the present gyrokinetic oscillators continue to absorb generator power as they collapse. The coronal plasma may thus be a common modifying influence on the current waveform, reducing or removing the "inductive notch" expected from simpler treatments. Because of this extra energy sink, the comparison of theory and experiment is modified in the right direction and magnitude.

While there are many potential caveats to the development presented here as we consider the early time development of the corona, the detailed role of transit time effects and the microstability of the evolving distribution functions, the collisionless magnetoplasma corona treated here may be an important ingredient in many plasma radiation sources, one that deserves close experimental attention.

ACKNOWLEDGMENTS

We acknowledge many helpful discussions with Ira Bernstein.

Support by the Defense Nuclear Agency for this work is gratefully acknowledged, and in particular the use of the PIC code MAGIC.

APPENDIX: DEVELOPMENT OF SELF-SIMILAR SOLUTIONS

Because the electrical properties of collisionless plasma are generally determined by a few moments of the distribution function, a convenient path to developing the constitutive relation $\mathbf{j}(\mathbf{E})$ is to examine the moment relations of the gyrokinetic equation. Only four parameters are, in fact, required to determine the response of the system. Each of these is based on a particular moment of the distribution function. For example, using the variables of the main text, energy conservation is expressed by the statement

$$\mathbf{j} \cdot \mathbf{E} = \frac{d\mathcal{E}}{dt} + \mathbf{v} \cdot \mathbf{F}, \quad (\text{A1})$$

where the pressure force is $\mathbf{F} = -\nabla \cdot \mathbf{P}$, and \mathbf{P} is the pressure tensor. Two of the basic parameters are already obvious in the two independent pressure tensor components, the others arise as shown below.

The macroscopic quantities that enter into the fluid (moment) equations are averages over the particle distribution function. The distribution functions that solve the gyrokinetic equations contain a class of separable functions of the form $g(r, t)F(\mu, p_\theta, r_0)$. Here, instead of writing the distribution in terms of the velocity components in cylindrical geometry, it is better to use the dynamical invariants, the magnetic moment μ , and the angular momentum p_θ . The two equivalent representations of the gyroaveraged distribution function are connected by

$$f(r, \mathbf{v}, t) = [m^2 r / 2\pi B(r, t)] n(r, t) F(\mu, p_\theta, r_0). \quad (\text{A2})$$

The factor in $[\dots]$ is the Jacobian of the transformation from \mathbf{v} to μ, p_θ , and ϕ the gyrophase. Without collisions the invariants for each particle do not change, and the velocity function F is constant in time along a guiding center trajectory, $r(r_0, t)$. The particle density $n(r, t)$ is no longer part of F , which is normalized as

$$\left(\frac{m^2 r_0}{2\pi B_0(r_0)} \right) \int d\mu dp_\theta F(\mu, p_\theta, r_0) = 1, \quad (\text{A3})$$

for both electrons and ions. With the assumption of quasineutrality the mass density ρ is $\rho = (Zm_{\text{elec}} + m_{\text{ion}})n(r, t)$.

Without collisions the distribution function is not necessarily Maxwellian. Instead, the distribution function should be computed by modeling the transition between the collisional and the collisionless plasma. While this is a complicated problem, outside the limited scope of this paper, the general result²⁴ is a tenfold increase in mean kinetic energy before the electrons become collisionless. Here the distribution function is viewed as an input to the problem.

The parallel pressure is defined through the average value of p_θ ,

$$r^2 P_{\parallel} = \rho L_{\parallel}^2 = \rho \int d\mu dp_\theta F \frac{p_\theta^2}{m^2}, \quad (\text{A4a})$$

and the perpendicular pressure becomes

$$P_{\perp} = \rho B M_{\perp} = \rho B \int d\mu dp_\theta \frac{F \mu}{m}. \quad (\text{A4b})$$

Here, and in other moments, the summation over species is implicit.

The axial current density, defined by averaging of the axial drift velocity of the guiding center

$$nev_z \equiv \left(\frac{nc}{B} \right) \left(\frac{mv_\theta^2}{r} + mc \frac{D(E/B)}{Dt} - w_1 \frac{\partial \ln B}{\partial r} \right),$$

is then readily calculated by momentum balance to be

$$J_z = \frac{\rho c^2}{B} \frac{D(E/B)}{Dt} + \frac{c}{B} \left(\frac{\rho L_{\parallel}^2}{r^3} - \frac{1}{r} \frac{\partial(r\rho B M_{\perp})}{\partial r} \right). \quad (\text{A5})$$

The first term is related to the acceleration of the $\mathbf{E} \times \mathbf{B}$ drift motion, the second comes from angular momentum conser-

vation, or P_{\parallel} , and the third is the magnetization contribution, from P_{\perp} . In the acceleration term the ions dominate; the electrons are more important for the two pressure-related terms, without thermal equilibrium between electrons and ions.

The fluid equation of motion in the radial direction, for an anisotropic pressure, includes a centrifugal force L_{\parallel}^2/r^3 that reflects the conservation of angular momentum,

$$\rho \frac{DU}{Dt} = \frac{\rho L_{\parallel}^2}{r^3} - \frac{1}{r} \frac{\partial(rpBM_{\perp})}{\partial r} - J_z B. \quad (A6)$$

An isotropic pressure implies that the collisions are sufficiently frequent to keep the velocity components randomized. The frequent collisions imply a finite conductivity, in contrast to the assumption of infinite conductivity, in ideal hydromagnetic theory, which demands a collisionless plasma. One might argue that pressure isotropy has been reached on time scales longer than those of interest, or as an initial condition. However, in a cylindrical geometry, as the plasma gets closer to the axis the pressure P_{\parallel} parallel to the magnetic field $B = B_{\theta}(r)$ increases as $1/r^2$, while the perpendicular pressure P_{\perp} increases as $1/r$. Thus the anisotropy is intimately connected to the time scale of interest in a collisionless cylindrical plasma.

In this gyrokinetic description the Maxwell–Vlasov system, as completed by the momentum balance including the anisotropic pressure P , can be summarized in the following equations:

$$\frac{\partial n}{\partial t} + \nabla \cdot (n\mathbf{W}) = 0, \quad (A7a)$$

$$\frac{\partial \mathbf{B}}{\partial t} = \nabla \times (\mathbf{W} \times \mathbf{B}), \quad (A7b)$$

$$\nabla \times \mathbf{B} = \frac{4\pi \mathbf{J}}{c} + \frac{1}{c} \frac{\partial \mathbf{E}}{\partial t}. \quad (A7c)$$

The displacement current is retained in the analysis in order to make connection with external power sources or sinks. For a cylindrically symmetric geometry the nonvanishing dependent variables are the fluid density ρ , the radial component of the fluid velocity $W_r = cU$, the axial component of the current density $J_z = J$, the azimuthal component of the magnetic field $B_{\theta} = B$, and the parallel and perpendicular moments L_{\parallel} and M_{\perp} .

In the limit of homogeneous compression ($U \propto r$), special initial conditions in these variables allow the equations to simplify. The dependent variables and their derivatives are then functions of the single self-similar invariant $\xi = r/r_0 \alpha(\tau)$. Here r_0 is a dimensionless scale length that arises directly in the transformation, viz., $r_0 \equiv \omega_E/\omega_A = r_0/l_0$ with $ct_0 = l_0$ and $\tau = t/t_0$. The time scale t_0 is a free parameter only to the extent that a particular implosion time scale for the core plasma remains arbitrary. The variable $\alpha(\tau)$ contains the sole time dependence, e.g., $U = \dot{\alpha}r_0$, $DU/D\tau = \ddot{\alpha}r_0$.

A self-similar oscillation is possible only when the accelerations are proportional to the pinch radius. For an isotropic pressure the proportionality of $J_z B_{\theta}/n$ to radius implies that the magnetic field is proportional to $\sqrt{\rho}$. In the anisotropic case additional profiles must be defined self-con-

sistently. Using Eq. (A7c) to eliminate J , and separating the four distinct spatial dependencies that arise, Eq. (A6) becomes

$$\ddot{\alpha} = \frac{\omega_{\parallel}^2}{\alpha^3} + \frac{\omega_{\perp}^2}{\alpha^2} - \frac{\omega_A^2}{\alpha} + \frac{\omega_E^2}{\alpha} \dot{\alpha}^2. \quad (A8)$$

The oscillatory term related to the magnetic field pressure is $-\omega_A^2/\alpha$, where $\tau_A = \omega_A^{-1}$ is the transit time of an Alfvén wave with velocity c_A through the pinch scale length r_0 , viz., $\omega_A^2 \equiv c_A^2/c^2 = B^2/4\pi\rho c^2$. As expected this term also occurs in the corresponding equation for the isotropic ideal hydromagnetic case. The two new terms related to the anisotropy are the parallel pressure term, with $\omega_{\parallel}^2 \equiv c_{\parallel}^2/c^2$, and the perpendicular pressure term, with $\omega_{\perp}^2 \equiv c_{\perp}^2/c^2$. The velocities c_A , c_{\parallel} , and c_{\perp} are thus alternate measures of the strengths of the fundamental moments in the theory, serving to parametrize the corresponding separation constants. Each dimensionless frequency ($\omega_k \equiv \tau_k^{-1}$) derives from a separate term in the momentum equation, and the velocity ratios obtain from the normalization of the moments to the light speed and the required dimensionality, viz., $L_{\parallel}^2 \sim l_0^2 c_{\parallel}^2 h_{\parallel}(\xi)$ and $BM_{\perp} \sim c_{\perp}^2 h_{\perp}(\xi)$. The final term, proportional to $\dot{\alpha}^2$, arises here only when we keep the full effects of displacement current; $\tau_E = \omega_E^{-1}$ is a measure of the overall dielectric strength characterizing any particular flow.

The four frequencies appearing in Eq. (A8) are connected to four constraint relations that define the required plasma profiles for enclosed current $I(\xi) = (cl_0 r_0/2)\xi B_0(\xi)$, number density $n_0(\xi)$, perpendicular (kinetic) temperature $h_{\perp}(\xi)$, and parallel (kinetic) temperature $h_{\parallel}(\xi)$. With the dielectric coefficient $\epsilon(\xi)$ given by

$$\epsilon(\xi) = \sqrt{1 + (4\pi m_i c^2) n_0(\xi) / B_0^2(\xi)}, \quad (A9a)$$

the constraints are given by

$$\omega_{\parallel}^2 = (c_{\parallel}^2/c^2) h_{\parallel}(\xi) [1 - 1/\epsilon^2(\xi)], \quad (A9b)$$

$$\omega_{\perp}^2 = -(c_{\perp}^2/c^2) \{ [1 - 1/\epsilon^2(\xi)] / r_0^2 \xi^2 n_0(\xi) \} \partial_{\xi} [\xi n_0(\xi) h_{\perp}(\xi)], \quad (A9c)$$

$$r_0^2 = [1 + \xi \partial_{\xi} \ln B_0(\xi) / \epsilon^2 \xi^2], \quad (A9d)$$

$$1 = [2 + \xi \partial_{\xi} \ln B_0(\xi)] / \epsilon^2. \quad (A9e)$$

These equations require $\omega_E < 1$ to obtain positive definite number density profiles and offer bounded solutions for each of the variables, usually over a finite range $[\xi_<, \xi_>]$. The spatial range used can be chosen to fit whatever physical dimensions are imposed because these solutions are simply following the motion of the single particle gyrokinetic trajectories. In other words, clipping these solutions in radius is admissible as long as the profile values and derivatives on the interior of any such domain limit to the proper values as one approaches the boundary.

¹ N. R. Pereira and J. Davis, *J. Appl. Phys.* **64**, R1 (1988).

² J. Pearlman and J. C. Riordan, *Proc. SPIE* **537**, 102 (1985); also see Fig. 5 in Ref. 1.

³ J. W. Thornhill, K. G. Whitney, and J. Davis, *J. Quant. Spectrosc. Radiat. Transfer* **44**, 251 (1990).

⁴ G. Merkel and D. A. Whittaker (private communication).

- ⁵ F. C. Young (private communication).
- ⁶ R. W. Clark, J. Davis, and F. L. Cochran, *Phys. Fluids* **29**, 1971 (1986).
- ⁷ F. L. Cochran (private communication).
- ⁸ I. B. Bernstein and P. J. Catto, *Phys. Fluids* **28**, 1342 (1985).
- ⁹ F. S. Felber, *Phys. Fluids* **25**, 643 (1982).
- ¹⁰ R. C. Davidson, *Phys. Fluids* **27**, 1804 (1984).
- ¹¹ R. C. Davidson, *The Theory of Non-Neutral Plasmas* (Benjamin, Reading, MA, 1974).
- ¹² R. J. Briggs, J. D. Daugherty, and R. H. Levy, *Phys. Fluids* **13**, 421 (1970).
- ¹³ R. H. Levy, *Phys. Fluids* **8**, 1288 (1965).
- ¹⁴ M. S. di Capua, *IEEE Trans. Plasma Sci.* **PS-11**, 205 (1983).
- ¹⁵ A. Ron, A. Mondelli, and N. Rostoker, *IEEE Trans. Plasma Sci.* **PS-1**, 85 (1973).
- ¹⁶ R. V. Lovelace and E. Ott, *Phys. Fluids* **17**, 1263 (1974).
- ¹⁷ J. M. Creedon, *J. Appl. Phys.* **48**, 1070 (1977).
- ¹⁸ R. F. Benjamin, J. S. Pearlman, E. Y. Chu, and J. C. Riordan, *Appl. Phys. Lett.* **39**, 848 (1981).
- ¹⁹ M. Krishnan, C. Deeney, T. Nash, P. D. LePell, and K. Childers, in *Dense Z Pinches*, AIP Conf. Proc. 195 (AIP, New York, 1989), p. 17.
- ²⁰ C. Deeney, T. Nash, P. D. LePell, M. Krishnan, and K. Childers, in *Dense Z Pinches*, AIP Conf. Proc. 195 (AIP, New York, 1989), p. 55.
- ²¹ C. Deeney, T. Nash, P. D. LePell, K. Childers, and M. Krishnan, in *Dense Z Pinches*, AIP Conf. Proc. 195 (AIP, New York, 1989), p. 62.
- ²² J. W. Thornhill (private communication); and F. C. Young, S. J. Stephanakis, and V. E. Scherrer, *Rev. Sci. Instrum.* **57**, 2174 (1986).
- ²³ R. B. Spielman, R. J. Dukart, D. L. Hanson, B. A. Hammel, W. W. Hsing, M. K. Matzen, and J. L. Porter, in *Dense Z Pinches*, AIP Conf. Proc. 195 (AIP, New York, 1989), p. 3.
- ²⁴ R. E. Terry, in NRL Memorandum Report 6051, 1987, p. 49 ff. See AIP Document No. PAPS PFBPE-03-0195-101 for 101 pages of Naval Research Laboratory Memorandum Report 6051, "Advanced Concepts Annual Report 1986" from the NRL Plasma Radiation Branch to the Defense Nuclear Agency. Order by PAPS number and journal reference from American Institute of Physics, Physics Auxiliary Publication Service, 335 East 35th St., New York, NY 10017. The price is \$1.50 for each microfiche (98 pages) or \$5.00 for photo copies of up to 30 pages, \$0.15 for each additional page over 30 pages. Airmail additional. Make checks payable to the American Institute of Physics.